JOURNAL OF AIRCRAFT
Vol. 47, No. 4, July–August 2010

Design Optimization for Minimum Sound Radiation from Point-Excited Curvilinearly Stiffened Panel

Pankaj Joshi,* Sameer B. Mulani,† Sham P. Gurav,‡ and Rakesh K. Kapania§
Virginia Polytechnic Institute and State University, Blacksburg, Virginia 24061-0203

DOI: 10.2514/1.44778

With the development of manufacturing techniques such as the electron beam free form fabrication, a metal deposition technique that deposits metal in complex shapes on a metallic base plate, it has become easy to manufacture complex shapes such as panels with curvilinear stiffeners. Designing panels with predefined structural and acoustic response is the focus of the present work. Researchers have dealt with sizing optimization of panels with straight/curvilinear stiffeners for many years and it has been proven that in many cases the mass of a panel with curvilinear stiffeners is lesser than the mass of a panel with straight stiffeners for a complex loading such as biaxial compression with shear and transverse pressure. This work deals with sizing as well as placement optimization of panel with straight and curvilinear stiffeners for desired structural and acoustic response. For acoustic optimization, point-excited stiffened panels are designed for minimal sound radiation given the constraint on total mass of the structure. The developed framework for structural-acoustic optimization of point-excited stiffened panels can be extended to multipoint excitation to capture the realistic excitations such as turbulent boundary-layer pressure fluctuations. Finite element method is used for structural response of the structure for point excitation, and acoustic response is calculated using Rayleigh integral. The present work deals with external radiation problem where the acoustic medium is air. The effect of air on the vibrating structure is considered to be very small. Therefore, coupling between structural and acoustic response is neglected. To reduce the computational expense of structural-acoustic optimization, a new methodology for objective function evaluation is proposed and optimal design for minimum radiated acoustic power is discussed.

Nomenclature

a	=	length of the plate, m
b	=	width of the plate, m
C	=	damping matrix
F	=	external dynamic force, N
K	=	stiffness matrix
M	=	mass matrix
m	=	mass, kg
N_θ	=	number of discretization points on hemisphere in the direction of θ
N_ϕ	=	number of discretization points on hemisphere in the direction of ϕ
p	=	pressure at the data recovery point, N/m^2
S	=	surface area of the structure, m^2
v_n	=	surface normal velocity of the plate, m/s
W	=	radiated acoustic power, Watt

I. Introduction

DEVELOPMENTS in rapid manufacturing techniques have made it easier to manufacture complex shapes for practical applications. One such technique, called electron beam free form fabrication (EBF3), developed by NASA [1], has promising features to manufacture panels with curvilinear stiffeners. Kapania et al. [2] have shown that curvilinear stiffened panels might give lighter weight design than straight stiffened panels under certain design loads. Therefore, it is essential to have a computational environment to get optimum design for curvilinear stiffened panels meeting all the design constraints such as buckling, stress (von Mises stress should be less than yield stress) and displacements. The problem at hand becomes more complex when it is optimized for acoustic response. A number of studies have examined the minimization of sound power radiated from a vibrating structure using gradient-based recursive quadratic programming algorithms, such as the quasi-Newton method, sequential quadratic programing method, particle swarm optimization (PSO), genetic algorithms (GAs), and simulated annealing.

Designing quiet structures is gaining attention everyday as noise regulations around the world are getting more strict. To reduce the noise environment, aircraft manufacturer use two types of noise control techniques: active and passive; Grosveld et al. [3] and Elliot et al. [4]. Active noise control essentially involves the placement of loudspeakers and microphones throughout the passenger cabin or flight deck in conjunction with a control system. Active noise control is an appealing technique since it can be fitted to existing airframes without major structural modification. Passive noise control, by contrast, seeks to reduce cabin noise by the modification of the airframe structure itself. For example, this could be in the form of acoustic treatments added to the cabin walls. Designing quiet structures is a type of passive noise control and comes under the broad category of multidisciplinary design optimization (MDO) [5]. Because of high nonlinearity of MDO problems, it is very difficult to obtain a true optimum and it solely depends on the type of optimization algorithm selected to tackle the MDO task. Therefore, the first step in optimization algorithm selection is to decide whether a gradient or nongradient method should be used. Gradient methods have the advantage of typically converging on an optimal solution rapidly. The disadvantage of gradient methods is getting stuck at the local minimum in the design domain.

Koopmann and Fahnline [6] discussed material tailoring approach to design structures for minimizing sound power of structures. To implement a material tailoring strategy, it is first necessary to

Presented as Paper 2009-2649 at the 50th AIAA/ASME/ASCE/AHS/ASC Structures Conference, Palm Springs, CA, 4–7 May 2009; received 6 April 2009; accepted for publication 3 May 2010.

*Graduate Research Assistant, Department of Aerospace and Ocean Engineering. Student Member AIAA.
†Postdoctoral Research Associate, Department of Aerospace and Ocean Engineering. Member AIAA.
‡Postdoctoral Research Associate, Department of Aerospace and Ocean Engineering. Member AIAA.
§Mitchell Professor, Department of Aerospace and Ocean Engineering. Associate Fellow AIAA.

construct a model of the response of the structure in terms of the design (material) variables to be optimized. The structural model is then combined with an acoustic model to give the radiated sound power for the optimization analysis. The sensitivity of the sound power with respect to material design variable is used for structural-acoustic optimization resulting in an optimum material parameters (design variables) which minimize the power output of the structure. Koopmann and Fahnline [6] called a structure that has been tailored to radiate minimal acoustic energy a week radiator. Cunefare [7] and Naghshinesh et al. [8] were the first few, among many others, researchers to study the characteristics of weak radiators. They generated surface velocity distributions in frequency domain for planar radiating surfaces minimizing sound power using an optimization analysis. Material tailoring is then used to vibrate real structures as weak radiators and corresponding forces (input) are obtained. This is an inverse problem where an outcome is known but the source of excitation is unknown.

St. Pierre and Koopmann [9] used a more direct optimization process resulting in surface velocity profiles having the same characteristic as the weak radiators. Cunefare [7], Naghshineh et al. [8], and St. Pierre and Koopmann [9] reported that the acoustic power reduction was accomplished by surface velocity redistribution such that adjacent areas of high and low acoustic pressure on the boundary surface balance each other. A single area of balanced high and low acoustic pressure radiates sound as a dipole source [10] while an area of unbalanced high and low acoustic pressure radiates more like a monopole [10]. Thus changing radiation from a collection of monopole sources to a collection of dipole sources can bring a large change in power output.

In past, the optimization strategy to control radiation can be divided into two ways. One way is to raise the fundamental frequency as high as possible and attempt to move structural resonance out of the frequency range of interest. Raising the fundamental frequency is useful because planar structures radiate acoustic power very effectively at their lowest fundamental resonance. Olhoff [11–13], Watts and Starkey [14], Starkey and Bernard [15], and Ballinger et al. [16] applied this approach to control radiation from planar structures. Another way to optimize for radiation control is by changing the shape of the boundary surface, also known as shape optimization. Bennett and Smith [17] and Haftka and Gurdal [18] have addressed the structural shape optimization in their book and a survey paper, respectively. Bernhard and Smith [19] used shape optimization to reduce radiated sound power from the structures.

Belegundu et al. [20] and Hambric [21] reported that nongradient optimization methods are attractive compared with gradient methods for structural-acoustic optimization because of the presence of the multiple local minima. A Pareto/min–max multicriteria optimization approach was used by Akl et al. [22] to get optimal design of underwater shell structures by simultaneously minimizing the shell vibration, sound radiation, weight of the stiffening rings, and the cost of the stiffened shell simultaneously. Wang and Lee [23] used global acoustic and structural design sensitivities for a gradient-based optimization scheme to simultaneously reduce the weight and sound pressure level at observation points (field points) at three frequencies. To calculate structural and acoustic design sensitivities Wang and Lee [23] used energy variational formulations obtained using bending energy, membrane energy, transverse shear energy and mass.

Optimal structural design problems to reduce noise are highly nonlinear in design variables and acoustic response, so, the most conventional methods are difficult to apply. Jeon and Okuma [24] used PSO for optimal bending design of a vibrating plate to minimize noise radiation. Belegundu et al. [20] designed a baffled plate excited by single frequency and broadband harmonic excitation to minimize the radiated acoustic power using a gradient-based optimization algorithm. Lu-yun and De-yu [25] used FEM to obtain structural frequency response and boundary element method (BEM) for low-frequency acoustic radiation and genetic algorithm (GA) for structural-acoustic optimization assuming structural and acoustic response are uncoupled. Fourie and Groenwold [26] presented an application of particle swarm optimization algorithm (PSOA) to the optimal shape and size design with respect to static load. Fourie and Groenwold [26] reported that PSOA yielded better solutions than GAs for geometry optimization of simple truss structures. Hassan et al. [27] reported that PSO outperforms the GAs with high-efficiency differential when used to solve unconstrained nonlinear problems with continuous design variables and less efficiency differential when applied to constrained nonlinear problems with continuous or discrete design variables. They concluded that PSO uses less number of function evaluations than GA.

Constans et al. [28] showed that sound power reduction can be accomplished by optimal placement and sizing of small point masses in the semicylindrical shell structure using a simulated annealing algorithm. The optimal small point masses can alter the critical mode shapes to quieter modes of vibration for sound power reduction. The same approach is followed in the present work but we have incorporated the straight/curvilinear stiffeners instead of point masses and sizing and shape optimization is done for the panel with straight/curvilinear stiffeners. Kapania et al. [2], Mulani et al. [29], and Joshi et al. [30] were the first one to investigate the effect of curvilinear stiffeners and reported results for structural optimization of panels with straight/curvilinear stiffeners. They concluded that the role of curvilinear stiffeners become important to reduce the weight of the structure with complex loading such as biaxial compression with shear and transverse pressure. In their study, the sound radiation from the structure was not addressed.

The focus of the present work is to develop a structural-acoustic optimization framework for a point excited panel with straight/curvilinear stiffeners meeting the mass constraint. This is the first time structural-acoustic optimization is being carried out to design a panel with curvilinear stiffeners. Placement, orientation, and curvature of stiffeners might play an important role in minimization of sound power radiated from the stiffened panel. Therefore, placement, shape and sizing optimization is done in single step to reduce the radiated acoustic power from the point-excited straight or curvilinearly stiffened panels. Figure 1 shows one such panel which can be easily manufactured by the EBF3 technique [1] or computer controlled machining. The developed framework for a structure with point excitation can be extended to a structural-acoustic optimization framework for multipoint excitation such as transverse pressure. The developed framework for point excitation will also lead to multipoint excitation with auto and cross correlation between individual point

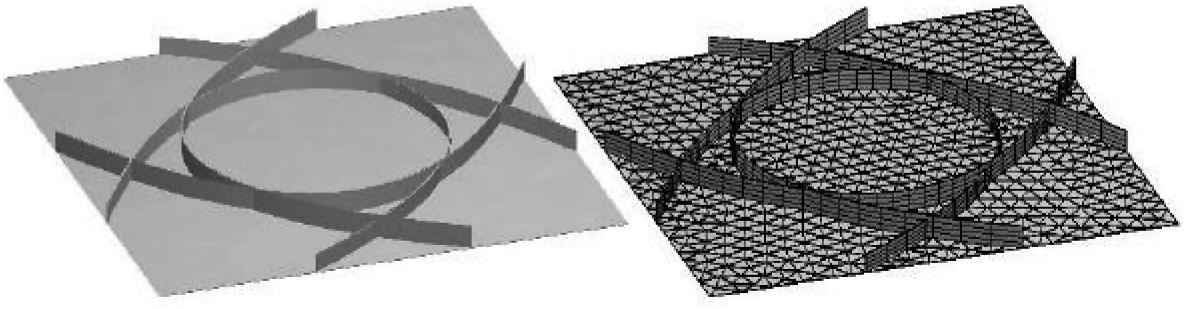

Fig. 1 *EBF*3 panel with curvilinear stiffeners and its finite element mesh [2].

excitations of structures thus making it capable to handling more realistic scenario such as excitation from turbulent boundary-layer pressure fluctuations.

Jeon and Okuma [24] used FEM for structural response, Rayleigh integral to calculate acoustic response and PSO as an optimization algorithm. They reported that PSO converged faster and gave better results than the optimization by steady state genetic algorithm. The present work uses SOL 108 of finite element analysis (FEA) software MD NASTRAN [31] for structural response, Rayleigh integral for acoustic response and an optimization tool VisualDOC [32], where PSO is being used as an optimization algorithm.

The work in the rest of the paper is discussed in six sections. Following the introduction, Sec. II explains the approach for structural and acoustic response calculation. Section III discusses the validation of Rayleigh integral approach for acoustic response calculation. The structural-acoustic optimization problem, addressed in this paper, deals with the frequency response calculation for point excitation with frequency varying from 10 Hz to 1000 Hz in the step of 2 Hz. Therefore, frequency response calculation becomes computationally expensive. To reduce the computational burden, a new approach for sound power calculation is discussed in Sec. IV. Section V deals with structural-acoustic optimization problem formulation. Results are reported in Sec. VI followed by conclusion and future work in Sec. VII.

II. Vibro-Acoustic Response Calculation

The structural vibration response analysis is the basis of structural-acoustic optimization. In the present work, the structural-acoustic optimization is carried out using a philosophy called noise-control-by-design [33] wherein the reduction of noise generated by structural vibration is treated as a design consideration. The sole aim of this design philosophy is to reduce the noise generated by the structure by changing design. To achieve this goal, optimization techniques are used and an optimal or suboptimal design is obtained. During the optimization process, structural and acoustic responses are calculated and sent to the optimizer. Structural and acoustic response calculations are discussed in following subsections.

A. Structural Response

The equation of motion for a multidimensional vibrating structure under dynamic load $F(t)$, if fluid medium influence is not considered, in the structures domain $\mathbf{\Omega^S}$, can be represented as

$$\mathbf{M}\ddot{\mathbf{U}} + \mathbf{C}\dot{\mathbf{U}} + \mathbf{K}\mathbf{U} = \mathbf{F}(t), \qquad x \in \mathbf{\Omega^S}, \qquad t > 0 \tag{1}$$

$\mathbf{U}$ is the nodal displacement vector matrix, $\mathbf{M}$ is the structural mass matrix, $\mathbf{C}$ is the viscous damping matrix, and $\mathbf{K}$ is the structural stiffness matrix. If we use harmonic excitation, $\mathbf{F}(t)$ can be expressed as

$$\mathbf{F}(t) = \mathbf{f}(\omega)e^{i\omega t} \tag{2}$$

where $f(\omega)$ is the magnitude of the harmonic load, ω is the frequency of excitation, and i is the imaginary number ($i^2 = -1$). The nodal displacement vector can be expressed as $\mathbf{U}(t) = \mathbf{u}(\omega)e^{i\omega t}$, where $\mathbf{u}(\omega)$ is the column matrix of the nodal complex displacement vectors. Time dependency of the dynamic problem can be eliminated using displacement vector and harmonic excitation in Eq. (2) and the frequency response equation, thus obtained, can be written as

$$\{-\omega^2\mathbf{M} + i\omega\mathbf{C} + \mathbf{K}\}\mathbf{u}(\omega) = \mathbf{f}(\omega) \tag{3}$$

In shorthand, the frequency response equation can be expressed as $\mathbf{A}(\omega)\mathbf{u}(\omega) = \mathbf{f}(\omega)$, where $\mathbf{A}(\omega) = -\omega^2\mathbf{M} + i\omega\mathbf{C} + \mathbf{K}$. Using Eq. (3), the nodal displacement vector matrix is written as

$$\mathbf{u}(\omega) = \mathbf{A}^{-1}(\omega)\mathbf{f}(\omega) \tag{4}$$

Using displacement vector, the velocity vector $\mathbf{v}(\omega)$ can be expressed as $\mathbf{v}(\omega) = i\omega\mathbf{u}(\omega)$. At the interface between the structure and the fluid with the assumption that the structure and the fluid are uncoupled, the nodal particle normal velocity vector can be written as

$$\mathbf{v_n}(\omega) = i\omega\mathbf{T}\mathbf{A}^{-1}(\omega)\mathbf{f}(\omega) \tag{5}$$

In Eq. (5), the $\mathbf{T}$ is a matrix of nodal vector normal to the surface of the structure. Finite element analysis tool MD NASTRAN [31] is used to calculate the nodal velocities as response to applied excitation for a range of frequencies from 10 to 1000 Hz in a step of 2 Hz. The nodal particle normal velocity is used as the input for acoustic response calculation.

B. Acoustic Response

This work deals with the external radiation problem where the external acoustic domain is air. The effect of the air on the structure will be small enough and can be neglected. Therefore, the structural and acoustic response are calculated independently and the coupling between structural and acoustic analysis has been neglected. The surface normal velocities obtained in Sec. II.A are used to calculate acoustic response of the structure using one of the two approaches discussed subsequently in this subsection. The first approach is to use BEM for acostic pressure calculation. The BEM [34] is a numerical integration technique employed in the determination of solutions to the acoustic wave equation for both interior and exterior acoustic fields. BEM approach requires normal velocities to be prescribed on the boundary of the fluid and structure interface, which consists of the nodes belonging to the mesh of the vibrating structure. A solution for the reduced-acoustic wave equation, or Helmholtz equation, is then sought which satisfies the imposed velocity boundary conditions obtained from structural analysis from Sec. II.A. The wave equation may be written in terms of a harmonic acoustic pressure field as [10]

$$\frac{\partial^2 p}{\partial x^2} + \frac{\partial^2 p}{\partial y^2} + \frac{\partial^2 p}{\partial z^2} + k^2 p = 0 \tag{6}$$

where p is the acoustic pressure, k is the acoustic wave number, and x, y, and z collectively define a Cartesian coordinate system. Acoustic wavenumber k is equal to ω/c, where ω is the angular frequency and c is the speed of sound in the acoustic medium. To determine the pressure throughout the acoustic medium, a solution to the Helmholtz equation [Eq. (6)] must be sought which satisfies the imposed normal velocity boundary conditions on the surface of the vibrating structure. It has been shown that the combination of the wave equation and the velocity boundary conditions on the vibrating surface results in the Kirchoff–Helmholtz integral equation [35], given by

$$p(\bar{r}) = \int_S \left[p(\bar{r}_s)\frac{\partial \tilde{G}(\bar{r}\bar{r}_s)}{\partial n} + j\omega\rho_0 v_n(\bar{r}_s)\tilde{G}(\bar{r}\bar{r}_s) \right] \mathrm{d}S \tag{7}$$

where $\bar{r}$ denotes a position vector, $\tilde{G}$ is the freefield acoustic Green's function, ρ_0 is the density of the acoustic fluid, v_n is the normal velocity over the surface S, and $\frac{\partial \tilde{G}}{\partial n}$ is the partial derivative of the acoustic Green's function with respect to the local outward normal n. The subscript s denotes the position vector of the noise source location on the surface of the vibrating structure. The freefield acoustic Green's function for a simple harmonic pressure field is given by

$$\tilde{G}(\bar{r}, \bar{r}_s) = \frac{e^{-jk|\bar{r}-\bar{r}_s|}}{4\pi|\bar{r}-\bar{r}_s|} \tag{8}$$

in which $|\bar{r} - \bar{r}_s|$ represents the magnitude of the vector $\bar{r} - \bar{r}_s$. Although Eq. (7) is written both in terms of the surface pressure $p(r_s)$ and the normal surface velocity v_n, a dependency exists between these quantities, simplifying the solution of this radiation problem [35].

For simple half-space radiation, the Kirchhoff–Helmholtz integral equation may be reduced to a more useful form that depends only on the surface velocity field of the radiating structure. It will be shown that the FEM mesh of a complex radiating structure provides a means for evaluating this reduced integral equation by approximating the integral with a summation over the elements of the FEM mesh. Thus,

each finite element is treated as a component source of the complex radiating structure. Furthermore, each of these component sources is small compared with the acoustic wavelength λ (maximum dimension $\ll \lambda$) which implies that such an analysis will appropriately model the phase variation of the radiated pressure, Kinsler et al. [36]. For baffled, planar radiators, a Green's function may be constructed for which $\frac{\partial \tilde{G}}{\partial n}$ is equal to zero over the entire radiating surface (Neumann boundary condition)

$$\tilde{G}(\bar{r}, \bar{r}_s) = \frac{e^{-jk|\bar{r}-\bar{r}_s|}}{2\pi|\bar{r}-\bar{r}_s|} \tag{9}$$

Thus, for this class of radiators, the pressure radiated to a point in the acoustic medium may be written solely in terms of the normal vibration of the radiating surface. This eliminates the complicated task of determining the surface pressure over the vibrating surface, which is required in the BEM approach. Removing the surface pressure component of the Kirchhoff–Helmholtz integral equation and substituting the half-space Green's function, the radiation of a baffled, planar structure is given by Rayleigh's integral [37] as

$$p(\bar{r}) = \frac{j\omega\rho_0}{2\pi} e^{j\omega t} \int_S \frac{v_n(\bar{r}_s) e^{-jk|\bar{r}-\bar{r}_s|}}{|\bar{r}-\bar{r}_s|} \, \mathrm{d}S \tag{10}$$

where $\bar{r}$ is the position vector of the point at which the pressure is being determined and $\bar{r}_s$ is the position vector locating a surface element of the vibrating structure as shown in the Fig. 2 [35]. *A* is the observation point in far field, *B* is the location of elemental noise source (simple source), *a* and *b* are the length and the width of the panel, respectively, and r, θ, and ϕ are spherical coordinate centered at the origin *O*.

In the second approach, the pressure is calculated using Rayleigh integral as shown in Eq. (10). The vibrational results are obtained by the FEM. From a FEM representation of a vibrating structure, the velocity of the structure at a number of defined nodal locations is known. Combining the nodal velocities with the knowledge of the structure's geometry, the normal surface velocity may be computed for each element comprising the structure. This discretized normal surface velocity suggests that Rayleigh's integral must be approximated by a summation over the elements comprising the complex structure. This discretization takes the following form:

$$p(\bar{r}) = \sum_{m=1}^{N} \frac{j\omega\rho_0}{2\pi} A_m v_m \frac{e^{-jkR_m}}{R_m} \tag{11}$$

where the index m identifies an element of the vibrating structure, N is the total number of elements, A_m is the area of the mth element, v_m is the normal velocity of the mth element, and R_m is the distance between the center of the mth element and the point in acoustic medium at which the pressure is to be evaluated. The variable v_m is calculated by taking the dot product of average elemental velocity at the centroid and the unit normal vector for the element under consideration. Average elemental velocity at the centroid of the element is calculated by averaging nodal velocities obtained using the FEM. Now, the radiated time average acoustic power W can be calculated as

$$W = \sum_{i=1}^{N_\theta} \sum_{j=1}^{N_\phi} \frac{|p(r, \tilde{\theta}_i, \tilde{\phi}_j)|^2}{2\rho c} r^2 \sin(\tilde{\theta}_i) \delta\theta\delta\phi \tag{12}$$

where

$$\delta\theta = \frac{\pi}{2N_\theta}; \qquad \delta\phi = \frac{2\pi}{N_\phi}; \qquad \tilde{\theta}_i = i\delta\theta; \qquad \tilde{\phi}_j = j\delta\phi \tag{13}$$

All of the information necessary for implementation of this approach is readily extracted from the FEM vibrational model. This method is most appropriately applied to planar, baffled radiators. In the present work we have used Rayleigh integral approach to calculate acoustic pressure.

III. Validation of Rayleigh Integral Approach

To validate the Rayleigh integral approach, a simply-supported rectangular plate as shown in Fig. 3 [38] is excited with a frequency varying point load of unit magnitude. Radiated acoustic power of the plate is calculated using Rayleigh integral approch and compared with the results available in the literature, Snyder and Tanaka [38]. Acoustic power calculated by Snyder and Tanaka [38] and Rayleigh integral approach is shown in Fig. 4. It is clear that the radiated acoustic power is close to the results of Snyder and Tanaka [38]. There is a shift in the plot of Snyder and Tanaka because Snyder and Tanaka used the modal superposition to calculate response and excited the plate at the corresponding frequency of that mode while we took the frequency from 50 to 125 Hz in the interval of 1 Hz. Other

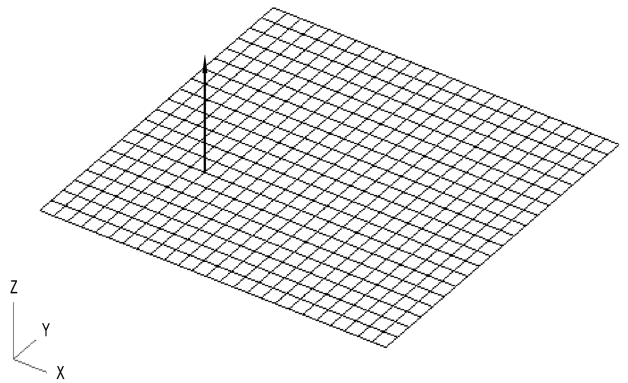

Fig. 3 FEM model of point excited simply supported rectangular panel used by Snyder and Tanaka [38].

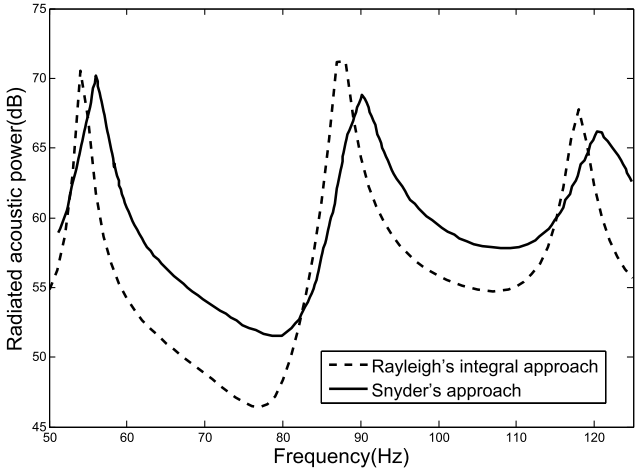

Fig. 4 Variation of radiated acoustic power with excitation frequency.

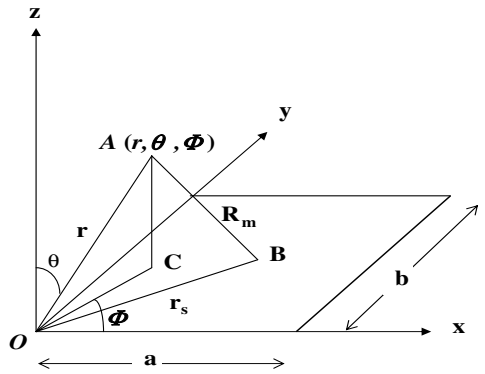

Fig. 2 Simply supported rectangular panel on the *x*-*y* plane with the origin at *O*.

than that, they approximated the integrand in sound power calculation using first two terms of MacLaurin series expansion. Thus, this comparison validates the Rayleigh integral approach for radiated acoustic power calculation. In the present work to calculate radiated acoustic power, velocities are being calculated by doing dynamic analysis of simply supported rectangular panel with two stiffeners at 495 frequencies starting from 10 to 1000 Hz with a step of 2 Hz. Finite element code MD NASTRAN [31] is used to calculate direct frequency response of panel with two stiffeners. Frequency response calculations at 495 frequencies make this process time intensive which in turn makes acoustic optimization computationally extremely expensive. Therefore, an approach is proposed here to reduce the computational burden. The proposed approach and the amount of reduction in CPU time are discussed in the following section.

IV. Frequency Response Function of Multidegrees of Freedom System via SDOF System

To reduce computational expense for vibro-acoustic optimization of a panel with two stiffeners, a general methodology is developed which is applicable to all linear structural vibration problems. The block diagram of this approach is shown in Fig. 5. In the proposed approach, the modeling and the mesh generation for the panel with two straight or curvilinear stiffeners is done in MD PATRAN first. Once, the finite element model is available, the modal analysis is carried out to extract natural frequencies between 10 to 1000 Hz using MD NASTRAN. These natural frequencies are then used to calculate damped natural frequencies (ω_d) for dynamic analysis of the stiffened panel. Structural damping is assumed to be 2%. Radiated acoustic power is calculated using velocities from dynamic analysis using Rayleigh integral approach. The area under radiated acoustic power vs frequency curve is calculated by representing each peak by frequency response function for the corresponding single degree of freedom system. The equation of motion of single degree of freedom system such as the mass-spring-damper is given as

$$m\ddot{x} + c\dot{x} + kx = F(t) \tag{14}$$

where m is the mass of the spring, c is damping coefficient, and k is the spring constant for a spring-mass-damper system. For harmonic excitation $F(t) = Ae^{j\omega t}$, the frequency response function $X(\omega)$ of the system is given as

$$X(\omega) = \frac{1}{\sqrt{\left\{1 - \left(\frac{\omega\sqrt{1-\zeta^2}}{\omega_d}\right)^2\right\}^2 + \left\{\frac{2\zeta\omega\sqrt{1-\zeta^2}}{\omega_d}\right\}^2}} \tag{15}$$

where ω is the frequency of excitation, ω_d is damped natural frequency of the corresponding mode, and ζ is the damping factor. To obtain frequency response function for a stiffened panel with harmonic point excitation, the dynamic analysis is being carried out at all ω_d and $C_1 * \omega_d$. C_1 is a factor which defines how well we are capturing each peak of the frequency response. Two unknowns A and ζ are calculated for each peak using Eqs. (16) and (17). Based on a parametric study it turns out that a value of $C_1 = 0.977$ captures the peaks of frequency response function (FRF) quite well. The area under frequency response curve is then used as an objective function in optimization and the goal is to minimize it while meeting mass constraints. The mass constraint in the present problem is the ratio of the mass of the structure being optimized to the mass of the base line structure. The baseline structure mass is obtained using structural optimization for uniaxial loading with shear under buckling constraint only

$$y(\omega, \zeta) = \frac{A}{\sqrt{\left\{1 - \left(\frac{\omega\sqrt{1-\zeta^2}}{\omega_d}\right)^2\right\}^2 + \left\{\frac{2\zeta\omega\sqrt{1-\zeta^2}}{\omega_d}\right\}^2}} \tag{16}$$

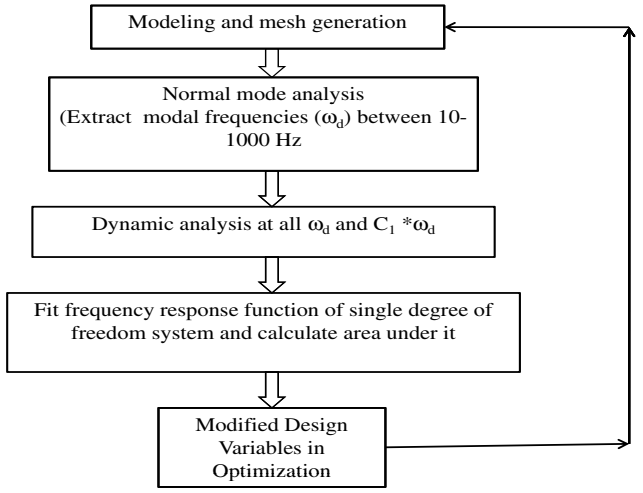

Fig. 5 Block diagram for proposed approach for structural-acoustic optimization.

$$y_{\max}(\zeta) = \frac{A}{2\zeta\sqrt{1-\zeta^2}} \approx \frac{A}{2\zeta} \tag{17}$$

where A is a constant and y is the response calculated at frequency of excitation ω_d. $y_{\max}$ is the maximum value of y obtained from Eq. (16) and it occurs at damped natural frequency ω_d. The proposed approach captures each peak of FRF quite well. Table 1 shows the comparison of the results obtained using the proposed approach and the regular dynamic analysis with 495 frequencies as described earlier. In the new proposed approach, we calculated response at 184 frequencies thus reducing the computational expense by 52.08%. This approach calculated response with 0.4% accuracy when compared with the regular dynamic analysis and it is acceptable for initial stage of optimization to reach rapidly to a region of optimum design.

V. Optimization Problem Formulation

A. Problem Definition

Optimization of acoustic response from a structure can be done using two approaches [39]. In the first approach, the response of a structure to the excitation is calculated and then the acoustic power radiated from the structure is obtained. Now, the design optimization cycle is carried out by changing the design variables. The second approach decouples the acoustic and structural domains. In the second approach the surface velocity profile of the structure for minimum acoustic response is found first and then the design variables are optimized to meet the desired velocity profile. In the present work, we have done the optimization using the first approach. In general, mathematically, we can define the optimization problem as follows:

$$\begin{aligned} &\min_x f(x) \qquad g_i(x) \le 1, \qquad i = 1, \cdots, m \\ &A_j \le x_j \le B_j, \qquad j = 1, \cdots, n \end{aligned} \tag{18}$$

Table 1 Comparison of results obtained using proposed approach

Approach	Frequency averaged radiated acoustic power, dB	Error in power, %	CPU time, min	% reduction (CPU time)
Proposed new approach	74.91	0.40	1.61	52.08
Regular dynamic analysis	74.61	——	3.36	——

As given in Eq. (18), f is the objective function that has to be minimized with respect to design variables x, while satisfying the constraints g_i shown in Eq. (18). The objective function f is the area under the radiated acoustic power versus frequency curve. g_1 is the mass constraint and for present problem m is one, i.e., we have only one constraint. The design variables indicated by vector x are subjected to constraints (often called as side constraints) in the form of upper limits (B_j) and lower limits (A_j). These are expressed in Eq. (18). Mathematical correlation to the optimization problem is explained in the following subsections.

B. Design Variables

The response of structures to a point excited harmonic load depend on the local mass, stiffness and damping. Thus by changing thickness of the plate, cross section of the curvilinear stiffeners and orientation of the stiffeners we can optimize the acoustic response. Thus we have thickness of the plate and the cross-sectional dimension of the stiffeners as design variables for sizing optimization. The main focus of the present work is to do placement and sizing optimization of panel with curvilinear stiffeners where we have taken into account the orientation of the stiffeners. All the 11 design variable $x_1, x_2, x_3 \cdots, x_{11}$ are shown in Fig. 6. The starting and the end point of the first stiffener are given by x_1 and x_2, respectively. Similarly, x_3 and x_4 are the starting and end point of second stiffener. The mid point for both the stiffeners are denoted by x_5 and x_6, respectively. The heights of the first and second stiffeners are represented by x_7 and x_8, respectively. The thicknesses of the first and second stiffeners are denoted by x_9 and x_{10} while x_{11} is the thickness of the plate. Therefore, the number of design variables have been increased from five for sizing optimization to 11 for both sizing and placement optimization.

C. Objective Function

There can be various possible objective functions for acoustic response of the panel with straight or curvilinear stiffeners. Potential candidates for the objective function for problems related to vibro-acoustic optimization are discussed as follows [40].

1. *Radiated Acoustic Sound Power*

The frequency average power over a frequency bandwidth is calculated using Eq. (12) at n_{freq} closely spaced frequency increments between $f_{\min}$ and $f_{\max}$ and can be expressed as

$$f = \tilde{W} = \frac{1}{f_{\text{span}}} \int_{f_{\min}}^{f_{\max}} W \, \mathrm{d}f \tag{19}$$

Frequency is varied from $f_{\min} = 10$ Hz to $f_{\max} = 1000$ Hz. f_{span} is given as the difference between $f_{\max}$ and $f_{\min}$. There was no constraint on the mass of the panel with curvilinear stiffeners.

2. *Radiated Acoustic Sound Power with Constant Mass*

For this case, the objective function is same as that used in the previous case except that we now have a constraint on the mass of the panel with curvilinear stiffeners. Mass of the whole structure is taken to be a constant value obtained by the optimizer meeting all the other requirements, such as buckling and stress.

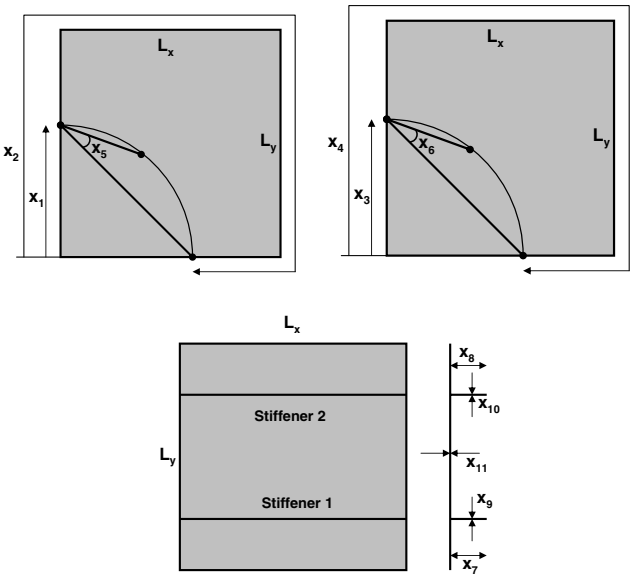

Fig. 6 Eleven design variables used in the optimization.

3. *Radiated Acoustic Sound Power with Constrained Mass*

Optimizing the structures for minimum radiated acoustic power may result in an increased mass of the structure. Therefore, for this case, an upper bound is put on the mass of the structure optimized for minimum radiated acoustic sound power. This constraint relationship for mass of the structure is given by Eq. (20)

$$g(x) = -1 + \frac{m_{\text{plate}}(x)}{m_{\max}} \tag{20}$$

where m_{plate} is the calculated mass for the present design and $m_{\max}$ is the upper bound on the mass of the whole structure.

4. *Mean Square Velocity*

An alternate formulation for objective function is taken to be frequency averaged mean square normal surface velocity of the structure. This objective function is less computationally expensive as there is no need to calculate Rayleigh integral to get the radiated acoustic power of the structure. The objective function can be expressed as follows:

$$f = \tilde{v} = \frac{1}{n_{\text{freq}}} \sum_{i=1}^{n_{\text{freq}}} \langle \bar{v}_{ni}^2 \rangle \tag{21}$$

In the present work, we have used the first objective function, i.e., frequency averaged radiated acoustic power for our optimization problem.

D. Constraints

Table 2 shows the constraints on the 11 design variables.

E. Baseline Stiffened Panel Design

Baseline panel is designed using developed optimization framework [41]. Baseline stiffened panel design optimization problem is

Table 2 Constraints in design variables

Design variable	Lower bound	Upper bound	Design variable	Lower bound	Upper bound
x_1	0.01 m	4.6636 m	x_7	0.01 m	0.1 m
x_2	0.01 m	4.6636 m	x_8	0.01 m	0.1 m
x_3	0.01 m	4.6636 m	x_9	0.001 m	0.020 m
x_4	0.01 m	4.6636 m	x_{10}	0.001 m	0.020 m
x_5	−30°	30°	x_{11}	0.001 m	0.01 m
x_6	−30°	30°	——	——	——

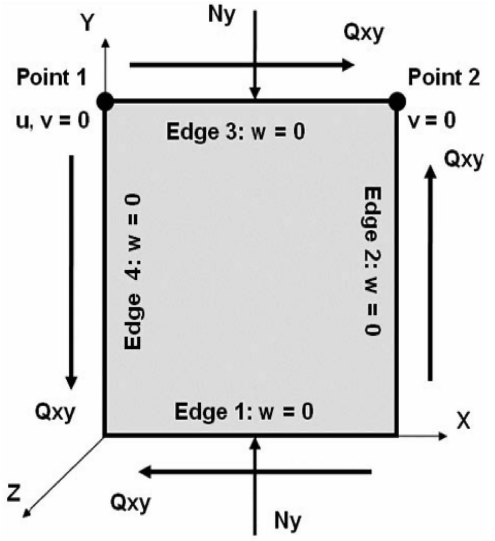

Fig. 7 Loads for baseline stiffened panel design.

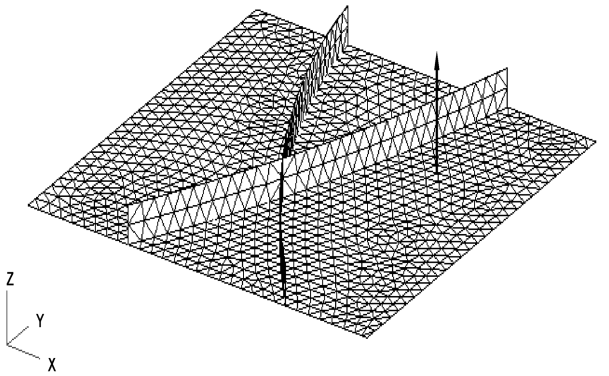

Fig. 8 Baseline design (1.1684 m × 1.1684 m) with unit excitation at (0.88 m, 0.73 m, 0).

solved for minimum mass meeting buckling and stress constraint. Stiffened panel is designed for the loading shown in the Fig. 7. Figure 8 shows the optimized baseline design for acoustic optimization. The optimized (minimum) mass for baseline panel is turned out to be 22.65 kg.

F. Optimizer and Optimization Framework

For the present optimization problem, a framework using PYTHON [42] (referred to as *EBF3PanelOpt*) has been developed [41]. This framework provides a flexibility of using either MD NASTRAN or ABAQUS for FEA. PYTHON scripts provide interfaces between the external optimizer and FEA as shown in Fig. 9. Commercial software VisualDOC [32] is used for optimization of acoustic response of stiffened panels. To locate a global minimum design with affordable computational expense, a combination of PSO and gradient-based optimization scheme (modified method of feasible directions) are used.

PSO is based on a social model that is closely tied to swarming theory [43]. According to Venter and Sobieski [44], particle swarm optimization makes use of a velocity vector to update the current position of each particle in the swarm. The position of each particle is updated based on the social behavior that a population of individuals, the swarm in the case of PSO, adapts to its environment by returning to promising regions that were previously discovered. The process is stochastic in nature and makes use of the memory of each particle as well as the knowledge gained by the swarm as a whole. Thus it explores the whole design space. Because of the complete domain search, it becomes expensive to get close to the narrow design space that contain the global minima. For a narrow design space, a gradient-based optimizer works better. Therefore, first PSO is used in VisualDOC to gather information about the whole domain as it randomly distributes the design variables in whole design domain. Once we have a rudimentary knowledge of the design domain containing a potential minimum, a refined search is done using VisualDOC with gradient-based optimizer in this smaller domain. Thus, the whole process becomes quite fast as we use the suboptimal design given by PSO as a starting point for gradient-based optimization in VisualDOC. Based on the given time constraint, we can distribute time for PSO to explore the design domain globally and then use gradient-based optimizer to explore design domain locally.

VI. Results and Discussion

Our objective is to reduce the frequency averaged radiated acoustic power given the constraint on the mass of a stiffened panel. The present structural-acoustic optimization problem covers frequency from 10 to 1000 Hz with a step of 10 Hz thus making it a very time intensive process. Therefore, based on the CPU time limitations, two optimal designs are obtained. First optimal design is obtained using PSO alone. Figure 10 shows the optimal design obtained using such an approach. In this case, PSO was stopped as it did not converge even after 59.5 hrs, although it gave a suboptimal design which met all the design constraints. In the second approach, a blending of PSO and gradient-based optimizers are used in sequence. Because of global exploration of design space, PSO gives an idea where the global optimal design might exist. Therefore, first the PSO is used for 4.92 hours to obtain a starting point for the gradient-based

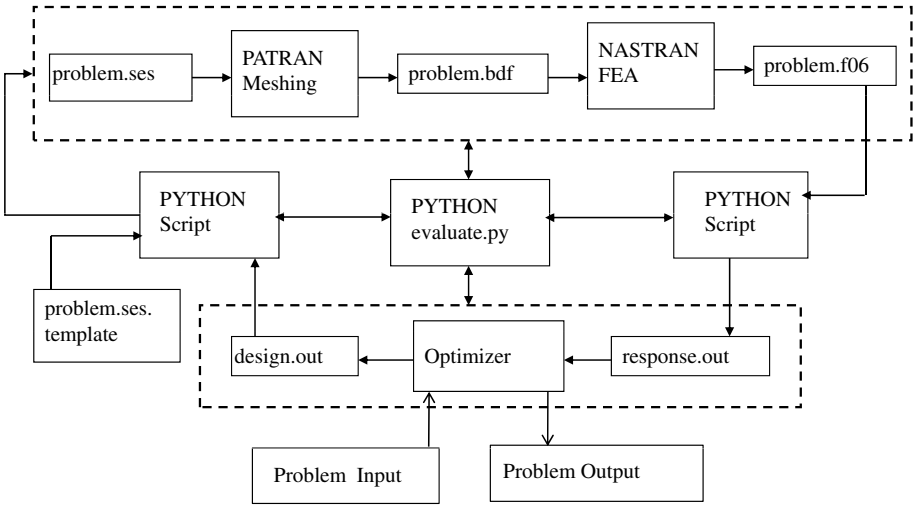

Fig. 9 Framework for optimization.

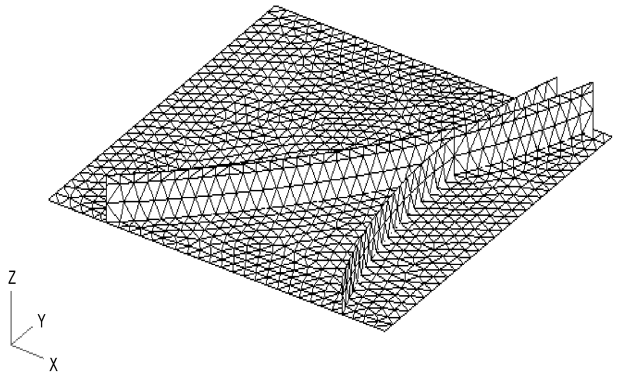

Fig. 10 Optimal design for acoustic response using particle swarm optimization.

optimizer. The time allocated for the PSO can vary, depending on the user's time constraint to obtain the optimal design. Figure 11 shows the optimal design obtained using a design obtained from PSO as a starting point for the gradient-based optimizer. The second approach took 6.78 hours including initial PSO run. Table 3 summarizes the results of two approaches. It is clear that if there is a time constraint, the second approach seems better as it takes lesser time to obtain an optimum design. If there is no time constraint, the first approach will give a better optimal design from acoustic response point of view with less mass. Another point to note is that the optimal design obtained using PSO alone gives a better design from acoustic point of view with lower structural strength than the design obtained using both PSO and gradient-based optimization algorithm. Therefore, from aircraft application point of view, the second design obtained using both PSO and gradient-based optimization algorithm will perform better as this design will have significantly lower acoustic radiation (compared with baseline design) with higher structural strength than the design obtained using PSO only.

From Figs. 10 and 11, it is clear that the placement optimization brings two stiffeners closer to the point of excitation, shown in Fig. 11, such that the stiffeners try to absorb energy from the source of excitation. Figure 12 shows the convergence history of frequency averaged radiated acoustic power of the panel with stiffeners. Mass constraint history is plotted in Fig. 13. As the mass of the structure reduces, it has higher velocity response thus radiating more acoustic power. Therefore, it is clear from Fig. 12 that the objective function, i.e., the frequency averaged radiated acoustic power increases first because the mass of the structure reduces during initial course of optimization. Frequency averaged total radiated acoustic power for our baseline design has a value of 74.6 dB which is optimized to 62.2 dB using first approach and to 66.9 dB using second approach. Mass constraint is satisfied in both cases and is close to 1, i.e., mass of base line design which is 22.65 kg. The response of optimal designs thus obtained using two approaches is compared with baseline

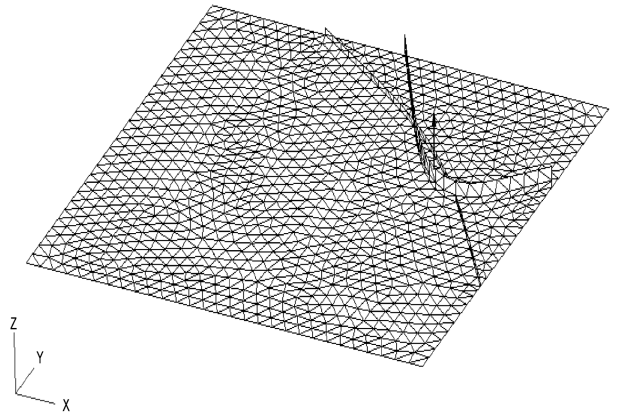

Fig. 11 Optimal design for acoustic response using combined PSO and gradient-based optimizer.

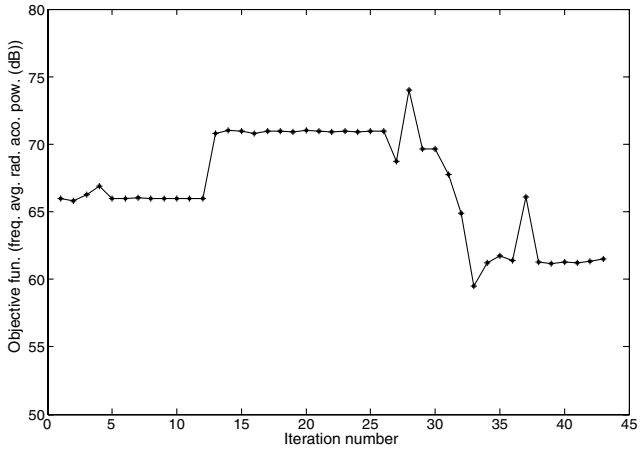

Fig. 12 Convergence history of frequency averaged radiated acoustic power using mixed (PSO + gradient-based optimization) algorithms.

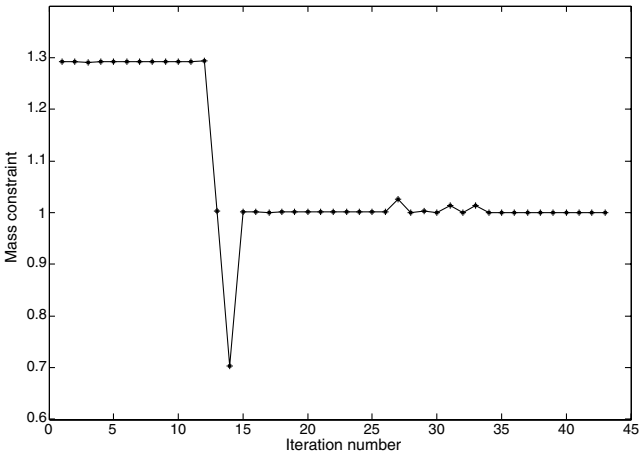

Fig. 13 Mass constraint history for the optimal design obtained using mixed (PSO + gradient-based optimization) algorithms.

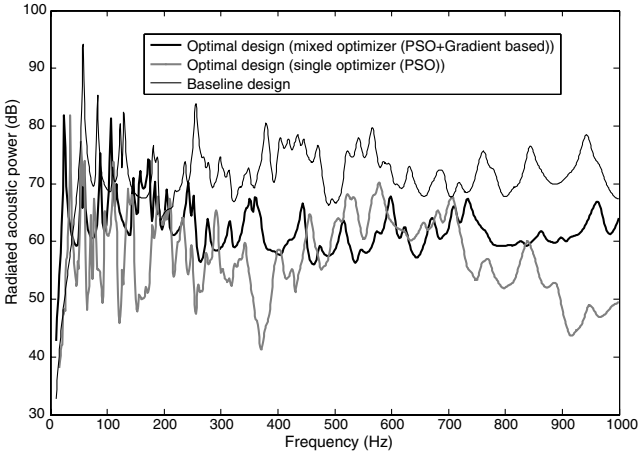

Fig. 14 Radiated acoustic power vs excitation frequency for baseline and optimal designs of curvilinearly stiffened panels.

design in Fig. 14. It is clear from Fig. 14 that the optimal designs have reduced the radiated noise from the structure significantly. Numerical values of all the 11 design variables for the baseline and two optimal designs are shown in Table 4. Figures 15–17 show the comparison of radiated acoustic power at different frequencies of excitation for baseline and two optimal designs, respectively, using two approaches. From Table 5, it is clear that the approximate objective

Table 3 Summary of structural-acoustic optimization results

Optimizer	Mass, kg	Frequency averaged radiated acoustic power, dB	Total time, h
PSO	13.55	62.2	59.5
PSO + gradient based	22.65	66.9	6.78

Table 4 Numerical values of design variables for baseline and two optimal designs

Design variables	Baseline design	Optimal design (PSO + gradient based)	Optimal design (PSO)
x_1	1.4860 m	2.6918 m	2.1543 m
x_2	3.6440 m	1.7371 m	3.520 m
x_3	2.040 m	3.1420 m	2.2790 m
x_4	4.1422 m	1.5024 m	4.2741 m
x_5	−7.52°	13.92°	−10.0°
x_6	3.56°	11.0°	7.59°
x_7	0.0839 m	0.0403 m	0.0807 m
x_8	0.0828 m	0.0130 m	0.10 m
x_9	0.0023 m	0.0194 m	0.0052 m
x_{10}	0.0024 m	0.0036 m	0.020 m
x_{11}	0.0056 m	0.0054 m	0.0010 m

Table 5 Comparision of objective function (frequency averaged radiated acoustic power) obtained using two approaches, 1) the proposed approach based on the single degree of freedom system, and 2) the regular approach based on Eq. (3)

Design	Objective function using proposed approach, dB	Objective function using regular approach, dB	Error, %
Baseline design	74.9	74.6	0.40
Optimal design (PSO + gradient based)	61.5	66.9	8.1
Optimal design (PSO)	63.5	62.2	1.99

function using proposed approach is close to the actual value of objective function and can be used to locate the optimum design somewhat rapidly.

VII. Conclusions

A methodology to approximately capture the response of a structure to dynamic point excitation is developed. Optimization results are obtained using this proposed methodology. A basis to choose two different optimization algorithm is also explored and it is concluded that from the aspect of total CPU time, blending of two optimization algorithms can give a suboptimal design quickly when compared with global optimization algorithm such as PSO. An overall reduction of 12.37 dB using first approach and that of 7.67 dB using second approach in frequency averaged radiated acoustic power is quite promising. At present the structure has been optimized for acoustic response putting mass constraint using baseline panel mass. Future work is to incorporate buckling constraint in the problem and do multi-objective optimization including mass as another objective function. This will require modelling of the effect of inplane loads on the structural dynamics of the stiffened panels as discussed recently by Schmidt and Frampton [45]. Deterministic and random pressure excitation will be incorporated in present vibro-acoustic optimization problem in future. Implementation of random pressure excitation, in-plane loads influence and buckling constraint

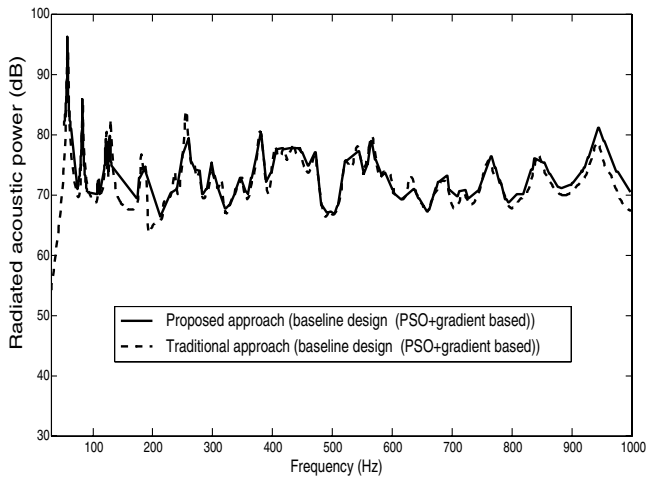

Fig. 15 Comparison of radiated acoustic power of baseline panel based on traditional and proposed approaches.

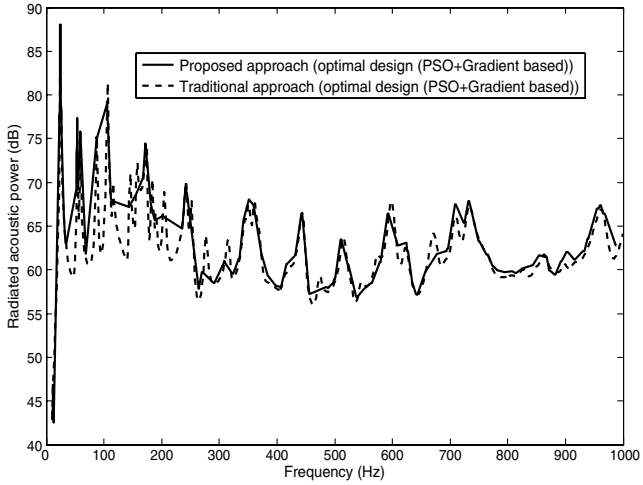

Fig. 16 Comparison of radiated acoustic power of optimized panel based on traditional and proposed approaches.

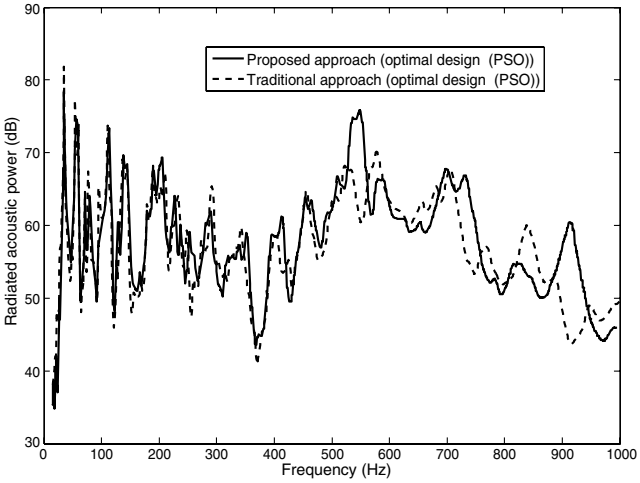

Fig. 17 Comparison of radiated acoustic power of optimized panel based on traditional and proposed approaches.

will bring design optimization problem to realistic situation. The capability of developed structural-acoustic optimization framework will be extended to handle curvilinear panels by integrating fast multipole BEM for acoustic calculations.

Acknowledgments

The work presented here is funded under NASA Subsonic Fixed Wing Hybrid Body Technologies National Research Announcement (NASA NN L08AA02C) with Karen Taminger as the associate principal investigator and Cynthia Lach as the contracting officer technical representative. We are thankful to both Karen Taminger and Cynthia Lach for their suggestions. The authors would like to thank other members of the *EBF*3 team and Dan Palumbo of the structural-acoustic branch at NASA Langley Research Center for technical discussions. Thanks are also due to our partners in the NASA National Research Announcement, Bob Olliffe, John Barnes, Dave Mavens, and Steve Englestadt, all of Lockheed Martin Aeronautics Company of Marietta, Georgia, for technical discussions.

References

[1] Taminger, K. M. B., and Hafley, R. A., "Electron Beam Freeform Fabrication: A Rapid Metal Deposition Process," *Proceedings of 3rd Annual Automotive Composites Conference*, Society of Plastics Engineers, Troy, MI, Sept. 2003.

[2] Kapania, R. K., Li, J., and Kapoor, H., "Optimal Design of Unitized Panels with Curvilinear Stiffeners," *AIAA 5th Aviation, Technology, Integration, and Operations Conference (ATIO)/16th Lighter-than-Air and Balloon Systems Conference*, AIAA, Reston, VA, 2005.

[3] Grosveld, F. W., Coats, T. J., Lester, H. C., and Silcox, R. J., "A Numerical Study of Active Structural Acoustic Control in a Stiffened, double Wall Cylinder," *Proceedings of NOISECON 94, National Conference on Noise Control Engineering*, Fort Lauderdale, FL, 1994.

[4] Elliot, S., Nelson, P., Strothers, I., and Bocher, C., "In-Flight Experiments on the Active Control of Propeller-Induced Cabin Noise," *12th Aeroacoustics Conference*, AIAA Paper No. 89-1047, San Antonio, TX, 1989.

[5] Padula, S. L., "Progress in Multidisciplinary Design Optimization at NASA Langley," NASA Langley Research Center, Rept. No. 107754.

[6] Koopmann, G. H. and Fahnline, J. B., *Designing Quiet Structures: A Sound Power Minimization Approach*, Academic Press, San Diego, CA, 1997.

[7] Cunefare, K. A., "The Design Sensitivity and Control of Acoustic Power Radiation by Three-Dimensional Structures," Ph.D. Dissertation, Pennsylvania State Univ., State College, PA, 1990.

[8] Naghshineh, K., Koopmann, G., and Belegundu, A., "Material Tailoring of Structures to Achieve a Minimum Radiation Condition," *Journal of the Acoustical Society of America*, Vol. 92, No. 2, Pt. 1, 1992, pp. 841–855. doi:10.1121/1.403955

[9] St. Pierre, R. L., and Koopmann, G. H., "Minimization of Radiated Sound Power From Plates Using Distributed Point Masses," *Proceedings of the ASME Winter Annual Meeting*, 93-WA/NCA-11, American Society of Mechanical Engineers, Fairfield, NJ, 1993.

[10] Pierce, A. D., "*Acoustics: An Introduction to its Physical Principles and Applications*," Acoustical Society of America, New York, 1989, pp. 159–166.

[11] Olhoff, N., "Optimal Design of Vibrating Rectangular Panels," *International Journal of Solids and Structures*, Vol. 10, No. 1, 1974, pp. 93–109. doi:10.1016/0020-7683(74)90103-6

[12] Olhoff, N., "A Survey of the Optimal Design of Vibrating Structural Elements. Part I: Theory," *The Shock and Vibration digest*, Vol. 8, No. 8, 1976a, pp. 3–10. doi:10.1177/058310247600800803

[13] Olhoff, N., "A Survey of the Optimal Design of Vibrating Structural Elements. Part II: Application," *The Shock and Vibration Digest*, Vol. 8, No. 9, 1976b, pp. 3–10. doi:10.1177/058310247600800903

[14] Watts, D., and Starkey, J., "Design Optimization of Response Amplitude in Viscously Damped Structures," *Journal of Vibration and Acoustics*, Vol. 112, 1990, pp. 275–280. doi:10.1115/1.2930505

[15] Starkey, J. M., and Bernard, J. E., "A Constraint Function Technique for Improved Structural Dynamics," *Journal of Vibration and Acoustics*, Vol. 108, 1986, pp. 101–106.

[16] Ballinger, R. S., Peterson, E. L., and Brown, D. L., "Design Optimization of a Vibration Exciter Head Expander," *Sound and Vibration*, April 1991, pp. 18–25.

[17] Bennett, J. A., and Smith, D. C., *The Optimum Shape: Automated Structural Design*, Plenum Press, New York, 1985.

[18] Haftka, R. T., and Gurdal, Z., "Structural Shape Optimization: A Survey," *Computer Methods in Applied Mechanics and Engineering*, Vol. 57, No. 1, 1986, pp. 91–106. doi:10.1016/0045-7825(86)90072-1

[19] Bernhard, R. J., and Smith, D. C., *Acoustic Design Sensitivity in Boundary Element Methods in Acoustics*, edited by R. D. Ciskowski, and C. A. Brebbia, Computational Mechanics Publications, New York, 1991.

[20] Belegundu, A. D., Salagame, R. R., and Koopmann, G. H., "A General Optimization Strategy for Sound Power Minimization," *Structural and Multidisciplinary Optimization*, Vol. 8, Nos. 2–3, 1994, pp. 113–119.

[21] Hambric, S. A., "Sensitivity Calculations for Broadband Radiated Acoustic Noise Design Optimization Problems," *Journal of Vibration and Acoustics*, Vol. 118, No. 3, 1996, pp. 529–532. doi:10.1115/1.2888219

[22] Akl, W., Ruzzen, M., and Baz, A., "Optimal Design of Underwater Stiffened Shell," *Structural and Multidisciplinary Optimization*, Vol. 23, No. 4, May 2002, pp. 297–310. doi:10.1007/s00158-002-0187-1

[23] Wang, S., and Lee, J., "Acoustic Design Sensitivity Analysis and Optimization for Reduced Exterior Noise," *AIAA Journal*, Vol. 39, No. 4, April 2001, pp. 574–580. doi:10.2514/2.1376

[24] Jeon, J., Y. and Okuma, M., "Acoustic Radiation Optimization Using the Particle Swarm Optimization Algorithm," *JSME International Journal Series C*, Vol. 47, No. 2, 2004, pp. 560–567. doi:10.1299/jsmec.47.560

[25] Lu-yun, C., and De-yu, W., "Structural-Acoustic Optimization of Stiffened Panels Based on a Genetic Algorithm," *Journal of Marine Science and Application*, Vol. 6, No. 4, Dec. 2007, pp. 55–61. doi:10.1007/s11804-007-7006-4

[26] Fourie, P. C., and Groenwold, A. A., "The Particle Swarm Optimization Algorithm in Size and Shape Optimization," *Structural and Multidisciplinary Optimization*, Vol. 23, No. 4, 2002, pp. 259–267. doi:10.1007/s00158-002-0188-0

[27] Hassan, R., Cohanim, B., Weck, O., and Venter, G., "A Comparision of Particle Swarm Optimization and the Genetic Algorithm," *46th AIAA/ASME/ASCE/AHS/ASC Structures, Structural Dynamics, and Materials Conference*, AIAA Paper 2005-1897, Austin, Texas, April 2005.

[28] Constans, E. W., Belegundu, A. D., and Koopman, G. H., "Design Approach for Minimizing Sound Power from Vibrating Shell Structures," *AIAA Journal*, Vol. 36, No. 2, 1998, pp. 134–139. doi:10.2514/2.7494

[29] Mulani, S. B., Li, J., Joshi, P., and Kapania, R. K., "Optimization of Stiffened Electron Beam Freeform Fabrication (EBF3) Panels using Response Surface Approaches," *48th AIAA/ASME/ASCE/AHS/ASC Structures, Structural Dynamics, and Materials Conference*, AIAA Paper 2007-1901, Honolulu, HA, 23–26 April 2007.

[30] Joshi, P., Mulani, S. B., Kapania, R. K., and Shin, Y. S., "Optimal Design of Unitized Structures with Curvilinear Stiffeners using

Response Surface Methodology," *49th AIAA/ASME/ASCE/AHS/ASC Structures, Structural Dynamics, and Materials Conference*, AIAA Paper 2008-2304, Schaumburg, IL, 7–10 April 2008.
[31] MD NASTRAN 2007 R2.1 Quick Reference Guide.
[32] VisualDOC, Design Optimization Software Version 6.1, Vanderplaats Research and Development, Colorado Springs, CO.
[33] Constans, E. W., Koopmann, G. H., and Belegundu, A. D., "The Use of Modal Tailoring to Minimize the Radiated Sound Power of Vibrating Shells: Theory and Experiment," *Journal of Sound and Vibration*, Vol. 217, No. 2, 1998, pp. 335–350. doi:10.1006/jsvi.1998.1799
[34] Estrof, O.von, *Boundary Elements in Acoustics: Advances and Application*, WIT Press, Southampton, United Kingdom, 2000.
[35] Fahy, F., *Sound and Structural Vibration*, Academic Press, New York, 1985.
[36] Kinsler, L. E., Frey, A. R., Coppens, A. B., and Sanders, J. V., *Fundamentals of Acoustics*, 3rd ed., Wiley, New York, 1982.
[37] Wallace, C. E., "Radiation Resistance of a Rectangular Panel," *Journal of the Acoustic Society of America*, Vol. 51, No. 3b, 1972, pp. 946–952.
[38] Snyder, S. D., and Tanaka, N., "Calculating Total Acoustic Power Output using Modal Radiation Efficiencies," *Journal of the Acoustic Society of America*, Vol. 97, No. 3, 1995, pp. 1702–1709. doi:10.1121/1.412048
[39] Denli, H., Frangakis, S., and Sun, J. Q., "Normalization in Acoustic Optimization with Rayleigh Integral," *Journal of Sound and Vibration*, Vol. 284, No. 3–5, 2005, pp. 1229–1238. doi:10.1016/j.jsv.2004.09.002
[40] Lamancusa, J. S., "Numerical Optimization Techniques for Structural-Acoustic Design of Rectangular Panels," *Computers and Structures*, Vol. 48, No. 4, 1993, pp. 661–675. doi:10.1016/0045-7949(93)90260-K
[41] Gurav, S. P., and Kapania, R. K., "Development of Framework for the Design Optimization of Unitized Structures," *50th AIAA/ASME/ASCE/AHS/ASC Structures, Structural Dynamics, and Materials Conference*, AIAA Paper 2009-2186, Palm Springs, CA, May 2009.
[42] Python 2.5.4, http://www.python.org
[43] Kennedy, J., and Eberhart, R., "Particle Swarm Optimization," *Proceedings of the IEEE International Conference on Neural Networks*, Perth, Australia, 1995, pp. 1942–1945.
[44] Venter, G., and Sobieski, J., "Particle Swarm Optimization," *43rd AIAA/ASME/ASCE/AHS/ASC Structures, Structural Dynamics, and Materials Conference*, AIAA Paper 2002-1235, Denver, CO, April 2002.
[45] Schmidt, P. L., and Frampton, K. D., "Effect of In-Plane Forces on Sound Radiation From Convected, Fluid Loaded Plates," *Journal of Vibration and Acoustics*, Vol. 131, No. 2, 2009. doi:10.1115/1.3025823.